Applied Catalysis A: General 452 (2013) 48–56

Contents lists available at SciVerse ScienceDirect

Applied Catalysis A: General

journal homepage: www.elsevier.com/locate/apcata

Pt-Mg-Ir/Al_2O_3 and Pt-Ir/HY zeolite catalysts for SRO of decalin. Influence of Ir content and support acidity

Silvana A. D'Ippolito, Laura B. Gutierrez, Carlos R. Vera, Carlos L. Pieck*

Instituto de Investigaciones en Catálisis y Petroquímica (INCAPE) (FIQ-UNL, CONICET), Santiago del Estero 2654, 3000, Santa Fe, Argentina

ARTICLE INFO

Article history:
Received 5 October 2012
Received in revised form
27 November 2012
Accepted 1 December 2012
Available online xxx

Keywords:
Selective ring opening
Decalin
Pt–Ir
Diesel

ABSTRACT

Pt-Ir/HY and Pt-Mg-Ir/Al_2O_3 catalysts were studied and tested in the reaction of ring opening of decalin. The acidity of the alumina support was modified by addition of 3% Mg and the acidity of the zeolite by ion exchange with NH_4Cl. The Pt content of the catalysts was fixed at 1% (mass basis) while the Ir content was adjusted between 0.1 and 0.6%. The catalysts were characterized by temperature programmed reduction, temperature programmed desorption of pyridine and FTIR of adsorbed CO. They were further tested with the reactions of cyclohexane dehydrogenation, cyclopentane hydrogenolysis and n-C_5 isomerization.

It was found that the Pt-Ir/HY catalyst was substantially more acid than Pt-Mg-Ir/Al_2O_3. Increasing the Ir content produced an increase of the hydrogenolytic activity and a decrease of the dehydrogenating activity of both catalysts. The n-pentane isomerization reaction results revealed that in the case of the alumina catalyst increasing the Ir content promoted both the catalyst stability and the cracking selectivity to C_5 isomers. The opposite was found for the Pt-Ir/HY zeolite catalysts. The zeolite supported Pt-Ir catalysts performed better for decalin ring opening than those supported on alumina. Higher Ir content favored the formation of ring-opening products in all cases.

1. Introduction

Selective ring opening (SRO) has been presented as a means of improving the quality of diesel fuel by increasing its cetane number (CN) and decreasing its density. The CN of naphthenic molecules is increased by converting rings into alkyl chains. Research works on SRO have mainly dealt with reactions of one-ring molecules despite the fact that two-ring molecules are more important to diesel chemistry. These are abundant in LCO (light cycle oil), a residual stream from the bottom of the fluid catalytic cracking (FCC) unit, commonly upgraded by hydrotreating in order to contribute to the diesel pool. Even in two-ring molecules the opening of only one ring does not lead to a substantial increase in the CN. Therefore for CN enhancement the opening of the second ring is crucial. Highly selective catalysts are needed for SRO of naphthenes since the cracking of C—C bonds of tertiary carbons should be involved if mainly linear products are to be obtained. Branched products have low CN [1].

Ring opening occurs by hydrogenolysis over certain noble metals [2] but proceeds more effectively on bifunctional catalysts [3]. It has been found that alumina supported metals such as Pt, Pd, Ir, Ru and Rh supported on Al_2O_3 are active and selective for ring opening of methylcyclopentane to C_6 paraffins [2,4]. McVicker et al. [5] emphasized the high activity and selectivity of Ir/Al_2O_3 catalysts for the ring opening of alkyl substituted cyclopentanes and bicycle C_5 naphthenes. When the acid function of the support is combined with the high hydrogenolytic activity of a noble metal, such as iridium, the resulting bifunctional catalyst is found to have an enhanced performance for SRO of naphthenes to alkanes [5]. The support acidity is essential for the opening of compounds having more than one ring, such as decalin, but not for compounds such as cyclohexane that can be opened using monofunctional metal catalysts [6]. Zeolites are a special kind of useful acid supports for this purpose. In this case the pore size and channel topology have a strong influence on diffusion and adsorption and hence on the final activity and selectivity for ring opening. Corma et al. [7] studied the conversion of decalin on zeolites of different pores sizes. HY, a big pore zeolite, is considered as one of the most appropriate supports for ring opening catalysts [7,8]. The zeolite crystal size [9] and the number and strength distribution of the acid sites [10,11] are important parameters for ring opening activity and selectivity. Kubicka et al. [11,12] determined that the acidity plays a very important roll in the SRO of bicycle naphthenes. Santikunaporn et al. [13] studied the contraction and ring opening of decalin and tetralin and they found that the Pt/HY catalysts are more effective than HY catalysts without metal promoter. The addition of Pt to USY zeolites is also found to greatly increase the rate of isomerization and therefore the formation of ring opening products. For

* Corresponding author. Tel.: +54 342 4533858; fax: +54 342 4531068.
E-mail address: pieck@fiq.unl.edu.ar (C.L. Pieck).

0926-860X/$ – see front matter © 2012 Elsevier B.V. All rights reserved.
http://dx.doi.org/10.1016/j.apcata.2012.12.002

these bifunctional metal-acid catalysts the formation of ring opening products increases with the proximity between the Pt and the acid sites and also with the increase of the metal/acid ratio [14].

Special classes of SRO catalysts are those based on two or more noble metals, such as Pt and Ir. For these systems the method of deposition of the metal is of crucial importance because a high metal-metal interaction is needed in the final catalyst for getting the desired modulation of the metal function properties.

Whereas classical coimpregnation and successive impregnation techniques lead to an unpredictable deposition of the two metals, other methods have been developed to favor the metal-metal interaction, such as the redox reactions in aqueous phase [15]. In this sense most works on Pt-Ir SRO catalysts focus their attention on catalysts prepared by common impregnation methods. Practically no works deal with SRO catalysts prepared by catalytic reduction. This preparation method has been previously reported to produce a strong interaction between the metals in naphtha reforming bimetallic catalysts [16–18]. A strong Pt–Ir interaction is known to enhance the hydrogenolysis reaction [19]. Pt-Mg-Ir(x)/Al_2O_3 catalysts prepared by catalytic reduction have been reported to have a strong interaction between Pt and Ir as confirmed by the presence of a Pt–Ir solid phase by electron diffraction [20]. Some patents propose that the addition of Mg has a beneficial effect on the performance of supported metal catalysts [21,22] though there is little information about this effect in the open literature.

The objective of this paper is to study the influence of the content of Ir, a metal with high hydrogenolytic activity, and the support acidity, on the SRO activity and selectivity of supported Pt–Ir catalysts. Decalin is used as a model naphthene molecule while HY zeolite and alumina are used as supports. Their acidity is modified by the addition of Mg (alumina) or the ion exchange with NH_4Cl (Y zeolite).

2. Experimental

2.1. Catalysts preparation

Pt–Mg/Al_2O_3 was prepared using an alumina supplied by Ketjen (CK-300, 200 $m^2\,g^{-1}$, 0.55 $cm^3\,g^{-1}$). This support was crushed and sieved in order to keep particles sizes between 35 and 80 mesh. Then it was calcined in flowing air at 500 °C for 4 h. Pt was added by a common impregnation method. An aqueous solution of HCl (0.2 mol l^{-1}) was added to the support and the system was left unstirred at room temperature for 1 h. Then an aqueous solution of H_2PtCl_6 (Sigma–Aldrich, 0.038 M) was added. The slurry was gently stirred for 1 h at room temperature and then it was put in a thermostated bath at 70 °C until a dry solid was obtained. The drying was completed in a stove at 120 °C overnight. The amount of the impregnating solution was adjusted in order to obtain 1.0 wt% Pt in the final catalyst. The Pt/Al_2O_3 catalyst was then calcined in flowing air at 300 °C for 4 h and cooled down to room temperature in nitrogen. A Mg doped of lower acidity was obtained by impregnation of Pt/Al_2O_3 with a solution of $Mg(NO_3)_2{\cdot}6H_2O$. The volume and concentration of this salt solution were adjusted to obtain a 3 wt% Mg on the final catalyst. Impregnation was performed by immersing the Pt/Al_2O_3 sample in the Mg solution and leaving the system unstirred for 1 h at room temperature. Then the slurry was dried in a thermostated bath at 70 °C until a dry solid was obtained. This solid was heated in a stove at 120 °C overnight. This Pt-Mg catalyst was finally calcined (air, 60 $cm^3\,min^{-1}$, 300 °C, 4 h) and reduced (H_2, 60 $cm^3\,min^{-1}$, 500 °C, 4 h) in a fixed bed reactor. A heating rate of 10 °C min^{-1} was employed for all heating steps. The Mg–Ir(0.6)/Al_2O_3 catalyst was made by the same procedure using an H_2IrCl_6 (0.08 M) solution instead of the H_2PtCl_6 one. The impregnation order was also changed. Mg was impregnated first and Ir last.

Pt-Mg-Ir(x)/Al_2O_3 catalysts were prepared by the catalytic reduction method using the Pt-Mg/Al_2O_3 catalyst as base support. Pt-Mg/Al_2O_3 was first reduced (H_2, 60 $cm^3\,min^{-1}$, 1 h, 300 °C, 10 °C min^{-1}) and then cooled down to room temperature in hydrogen. Then a degassed H_2IrCl_6 solution with the appropriate concentration was poured into the reactor. The catalyst-solution slurry was mildly stirred for 1 h while bubbling hydrogen (300 $cm^3\,min^{-1}$). Then the solution was drained and the catalyst was placed in a fixed bed, dried at 100 °C (hydrogen, 12 h, 60 $cm^3\,min^{-1}$, 2 °C min^{-1} heating rate) and reduced at 500 °C (hydrogen, 2 h, 60 $cm^3\,min^{-1}$, 2 °C min^{-1} heating rate). The Ir concentration of the impregnating solution was varied in order to obtain 0.1, 0.3 and 0.6 wt% Ir on the final catalysts. A total transfer of Ir from the solution to the catalyst was assumed. This was confirmed by ICP chemical analysis of the spent solution. The final catalysts were named Pt-Mg-Ir(x)/Al_2O_3 (x: nominal Ir content).

Pt-Ir(x) catalysts were prepared using a non-commercial NaY zeolite base support (Si/Al = 3.16, provided by the Petrobras R&D Center, CENPES). This zeolite was exchanged with an aqueous solution of NH_4Cl 2.2 M for 2 h at room temperature and with mild stirring. The solid was then filtered, repeatedly washed with distilled water and dried in an oven at 120 °C overnight. The dried solid was then calcined in air (2 h at 500 °C, heating rate 2 °C min^{-1}). The Si/Al ratio of the thus obtained material was 3.7 as measured by ICP chemical analysis. Pt and Ir were added by a common wet impregnation technique using H_2PtCl_6 and H_2IrCl_6 aqueous solutions. Pt and Ir monometallic catalysts were prepared by one-step impregnation and Pt-Ir by one-step coimpregnation. The metal concentration of the solutions was regulated in order to obtain the desired metal contents (Pt: 1.0 wt%; Ir: 0.1, 0.3 and 0.6 wt%). After the impregnation of the metals the samples were oven dried at 120 °C, calcined in dry air (3 h, 300 °C) and reduced in hydrogen (2 h, 300 °C). The thus obtained catalysts were named Pt-Ir(x)/zeolite (x: Ir mass content).

2.2. Temperature-programmed desorption of pyridine

This test was used for measuring the amount and strength of the acid sites. Samples of 200 mg were impregnated with an excess of pyridine. The samples were then rinsed and the excess of physisorbed pyridine was eliminated by heating the sample in a nitrogen stream at 110 °C for 1 h. Then the temperature was raised at a rate of 10 °C min^{-1} to a final value of 650 °C. To measure the amount of desorbed pyridine the reactor exhaust was connected to a flame ionization detector.

2.3. Temperature-programmed reduction (TPR)

The tests were performed in an Ohkura TP2002 apparatus equipped with a thermal conductivity detector. At the beginning of each TPR test the catalyst samples were pretreated in situ by heating in air at 400 °C for 1 h. Then they were heated from room temperature to 700 °C at 10 °C min^{-1} in a gas stream of 5.0% hydrogen in argon (molar base).

2.4. Fourier transform infrared (FTIR) absorption spectroscopy of chemisorbed CO

FTIR spectra of adsorbed CO were obtained in order to study the effect of Ir deposition on the properties of the metal function. The spectra of chemisorbed CO for the prepared catalysts were recorded within the wavenumber range of 4000–1000 cm^{-1}. A Shimadzu Prestige-21 spectrometer with a spectral resolution of 4 cm^{-1} was used. Spectra were recorded at room temperature and self-supported wafers with a diameter of 16 mm and a weight of 20–25 mg were used. The experimental procedure was as follows:

catalyst samples were reduced in a hydrogen flow at 400 °C (reached at a 10 °C min^{-1} heating rate) for 30 min. Samples were then degassed at 2.7×10^{-3} Pa and 400 °C for 120 min. After an initial (I) spectrum had been recorded, the samples were exposed to a CO pressure of 4000 Pa for 5 min and then a second (II) FTIR spectrum was recorded. The chemisorbed CO absorbance for each sample was obtained by subtracting spectrum I from spectrum II.

2.5. Cyclopentane hydrogenolysis

Before the reaction the catalysts were reduced for 1 h at 500 °C in hydrogen (60 cm^3 min^{-1}). Then they were cooled down in hydrogen to the reaction temperature (350 °C). The other conditions were: catalyst mass = 150 mg, pressure = 0.1 MPa, H_2 flow rate = 40 cm^3 min^{-1}, cyclopentane flow rate = 0.483 cm^3 h^{-1}. The products were analyzed in a Varian 3400 CX chromatograph equipped with a capillary column (Phenomenex ZB-1) and a flame ionization detector.

2.6. Cyclohexane dehydrogenation

The reaction was performed in a glass reactor with the following conditions: catalyst mass = 50 mg, temperature = 300 °C, pressure = 0.1 MPa, H_2 = 36 cm^3 min^{-1}, cyclohexane = 1.61 cm^3 h^{-1}. Before the reaction the catalysts were reduced in hydrogen (36 cm^3 min^{-1}, 500 °C, 1 h). The products were analyzed by capillary GC as described in the previous paragraph.

2.7. n-Pentane isomerization

The reaction was carried out for 4 h in a continuous flow glass reactor with the following conditions: atmospheric pressure, temperature = 400–500 °C, WHSV = 4.5, molar ratio H_2:n-C_5 = 6, catalyst mass = 100–150 mg. Before the reaction the samples were reduced in hydrogen at 500 °C for 1 h. The analysis of reactants and products was performed using the same procedure described in the previous paragraphs.

2.8. Selective ring opening (SRO) of decalin

All SRO experiments were performed in a stainless steel, stirred autoclave reactor. The reaction conditions were: temperature = 300–350 °C, hydrogen pressure = 3 MPa, stirring rate = 1360 rpm, volume of decalin = 25 , catalyst mass = 1 g. The used decalin was a mixture with a 37.5% of the *cis* isomer (*trans*/*cis* ratio of 1.63). It was found that the attrition action of the stirrer reduced the suspended catalyst to a powder that after drying would mostly pass through a 200 mesh sieve. This particle size and the high stirring rate ensured that diffusional limitations to mass transfer were eliminated. This was further confirmed by calculating the Weisz–Prater modulus ($\Phi = 0.06 << 1$). A sample was taken at the end of the experiments and it was analyzed using a Varian 3400 CX gas chromatograph equipped with a capillary column (Phenomenex ZB-5) and a flame ionization detector. Preliminary tests of identification of the products were performed by GC MS in a Saturno 2000 mass spectrometer coupled to a GC Varian 3800 using the same GC column.

3. Results and discussion

The TPR results are shown in Fig. 1. It can be seen that the TPR trace of the Pt-Mg/Al_2O_3 catalyst has two peaks of reduction; one at about 150 °C and a larger one at 203 °C with a shoulder at 340 °C. The first peak was attributed to the reduction of Pt oxides of big particle size whereas the peak at 203 °C was attributed to the reduction of more dispersed Pt oxide species [23]. The shoulder at 340 °C was assigned to the reduction of Mg species [24] catalyzed by Pt. The TPR trace of the Mg-Ir(0.6)/Al_2O_3 catalyst had a reduction peak at 150 °C due to the reduction of Ir oxide species and another reduction band at about 300–430 °C probably due to the reduction of Mg oxides. The higher reduction temperature and the small size of the peak of the Mg oxides show that there is no interaction between Ir and Mg. The addition of Ir to the Pt-Mg/Al_2O_3 catalyst produced a shift of the Pt reduction peak from 203 °C to smaller temperatures (172 °C) indicating a strong interaction between Pt and Ir. The effect of Mg (1 wt%) addition on the reduction of the alumina supported Pt(1 wt%)-Ir(x = 0.1, 0.3 and 0.6 wt%) catalysts has been previously reported [20]. It was found that Mg produces a decrease of the reduction temperature of both the Ir and Pt oxide species. This shift could be due to a lower Ir- or Pt-support interaction as a consequence of the lower acidity of the Mg doped supports. The addition of Mg also increases the electron density of Pt making its reduction easier [24,18]. Both Pt and Ir species are therefore reduced at a lower temperature.

In the case of the HY based catalysts, the Pt oxide species are reduced at a lower temperature than the Ir oxides. Moreover the Pt catalyst has a reduction zone at high temperatures (200–400 °C) that can be attributed to the reduction of Pt oxides highly dispersed on the support. Contrary to what was found for the catalysts supported on Al_2O_3 the addition of Ir to the monometallic Pt/zeolite catalyst produced a shift of the peak of reduction of Pt oxides from 169 °C to higher temperatures (205 °C). The Pt-Ir(0.3)/zeolite and Pt-Ir(0.6)/zeolite catalysts had only one peak of reduction, thus showing a strong interaction between Pt and Ir.

It is interesting to analyze why the Pt oxides are reduced at a lower temperature than the Ir oxides on the zeolite support while the Pt oxides are conversely reduced at a higher temperature than the Ir oxides on the alumina support. On the zeolite the Ir and Pt precursors are deposited on weak adsorption sites. As a consequence the reduction temperature depends mainly on the metal properties and the Pt oxides are reduced at lower temperatures than the Ir oxides [18]. On Al_2O_3 the Pt is deposited on the strong acids sites of Al_2O_3 producing Pt oxide surface species in strong interaction with the support. Ir impregnation is however done on alumina that has been previously doped with Mg. Therefore Ir is deposited over sites with low interaction and the Ir oxides are reduced at a low temperature. Something similar occurs when Pt is deposited over alumina or silica. In the first case Pt species in strong interaction with the support are reduced at about 230–260 °C while Pt oxides on SiO_2 are reduced at 100–150 °C due to the weak Pt–SiO_2 interaction [25].

From the TPR results it can thus be concluded that Pt and Ir are in strong interaction on both supports.

The pyridine TPD results are shown in Fig. 2. It can be seen that the concentration of strong acids sites of the Pt-Mg-Ir(x)/Al_2O_3 series is smaller than that of the Pt-Ir(x)/zeolite. Acidity values relative to Pt-Mg/Al_2O_3 and a classification of acids sites regarding their strength are included in Table 1. The results indicate that the total acidity of the catalysts supported on the HY zeolite is approximately 20 times greater than that of the Mg doped alumina. It can be seen that Mg decreases the acidity of the alumina due to their strong basic character, the moderate strength acidity being more affected. Given the acid character of Ir the addition of this metal causes an increase of the amount of moderate acid sites while decreasing the amount of weak acid sites of the Al_2O_3 catalysts. In the case of the Pt-Mg-Ir(x)/Al_2O_3 series the total acidity is slightly decreased by Ir addition because Ir species replace preexisting surface Cl groups. The total acidity of the zeolite catalysts is modified less by the addition of Ir, the acidity being slightly increased after Ir addition. 100% of the acid sites are strong in the case of the zeolite supported catalysts.

The influence of Pt and Ir addition on the acidity of the zeolite catalysts was studied by FTIR absorption experiments. Fig. 3 shows

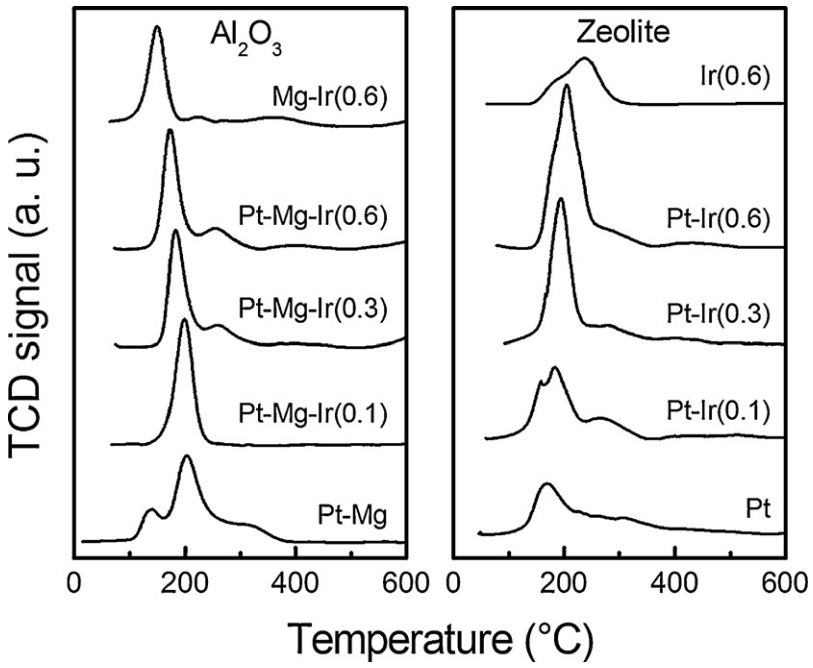

Fig. 1. TPR profiles of monometallic catalysts and Pt-Mg-Ir(x)/Al_2O_3 and Pt-Ir(x)/zeolite series.

the FTIR spectra of the OH region. The OH species attributed to Brønsted acid sites have two bands at 3557 and 3637 cm^{-1} due to different positions into the zeolite [26–28]. The bands at 3672 and 3735 cm^{-1} are attributed to extra-framework entities, extra framework Al atoms (EFAls) and silanols. The spectrum changes drastically after the addition of metals (Ir and/or Pt). Brønsted acid sites are redistributed in the monometallic samples. The OH FTIR bands become weaker and concentrated at 3603 cm^{-1}. Signals due to EFAls and silanols remain unchanged.

In the case of the bimetallic catalyst a quite different spectrum is obtained. The band due to OH groups disappears but another envelope appears that suggests the presence of OH species dispersed in the matrix, modified by the presence of the metallic particles, probably interacting with each other.

The interaction between the metals was also studied by FTIR-CO spectroscopy. Fig. 4 shows the IR spectra at 30 Torr in the 1850–2250 cm^{-1} wavelength range for the Pt-Mg/Al_2O_3, Pt-Mg-Ir(0.6)/Al_2O_3 and Mg-Ir (0.6)/Al_2O_3 catalysts. CO is adsorbed on Pt particles in the linear and bridge forms. In Fig. 4 only the wavenumber region corresponding to linear CO is shown, because the band due to CO adsorbed in the bridge form, Pt_2CO, was too small to be studied. The band at 2070 cm^{-1} corresponds to the adsorption of

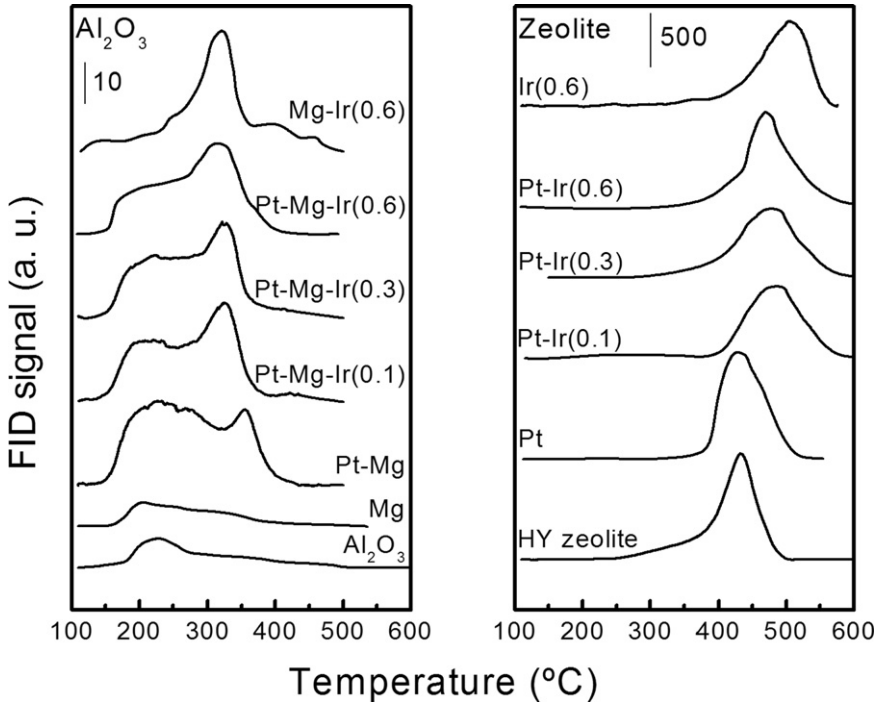

Fig. 2. Pyridine TPD results. Monometallic catalysts, Pt-Mg-Ir(x)/Al_2O_3 catalysts, Pt-Ir(x)/zeolite catalysts and supports.

Table 1
Values of the area of the pyridine TPD trace (relative to the area of the TPD trace of the Pt-Mg catalyst). Classification of acid sites according to their strength.

Catalyst	TPD area	Acid sites distribution (%)		
		Weak ($T < 300\,^{\circ}C$)	Moderate ($300 < T < 400\,^{\circ}C$)	Strong ($T > 400\,^{\circ}C$)
Al_2O_3	0.28	42	58	–
Mg/Al_2O_3	0.24	69	31	–
$Pt\text{-}Mg/Al_2O_3$	1.00	72	28	–
$Pt\text{-}Mg\text{-}Ir(0.1)/Al_2O_3$	0.88	53	47	–
$Pt\text{-}Mg\text{-}Ir(0.3)/Al_2O_3$	0.86	43	57	–
$Pt\text{-}Mg\text{-}Ir(0.6)/Al_2O_3$	0.84	40	60	–
$Mg\text{-}Ir(0.6)/Al_2O_3$	0.81	31	69	–
HY zeolite	21.51	–	38	62
Pt/zeolite	22.68	–	–	100
Pt-Ir(0.1)/zeolite	20.92	–	–	100
Pt-Ir(0.3)/zeolite	21.44	–	–	100
Pt-Ir(0.6)/zeolite	21.80	–	–	100
Ir(0.6)/zeolite	21.93	–	–	100

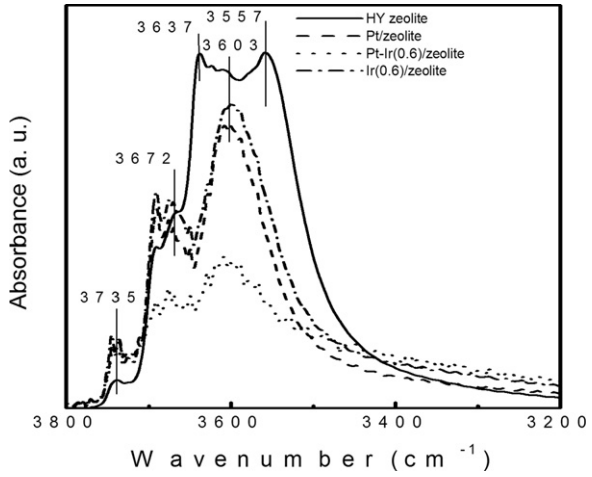

Fig. 3. FTIR OH-stretching bands of the Pt/zeolite, Pt-Ir(0.6)/zeolite and Ir(0.6)/zeolite catalysts. Comparison with HY zeolite.

linear CO on Pt [29–32]. Adsorption of CO on Ir/Al_2O_3 was studied by Solymosi et al. [33]; they attributed a band at 2080–2050 cm^{-1} to the presence of Ir^0–CO complexes.

The band at 2188 cm^{-1} in the spectra of the three catalysts studied can be assigned to the interaction between CO and Al_2O_3 [34,35]. It is specifically associated to adsorption on alumina Lewis acid sites, Al^{3+} ions with tetrahedral coordination [36–39]. This band disappears upon evacuation (results not shown) as reported elsewhere [37]. In Fig. 4 the characteristic peaks due to carbonyls on Mg^{2+} ions cannot be found. This is shown in greater detail in Fig. 4(a); the trace in the inset is the enlarged FTIR absorption spectrum of CO on Mg/Al_2O_3 in the 2250–2150 cm^{-1} range, where bands due to Mg^{2+} are expected. They are usually found in the 2213–2144 cm^{-1} range and correspond to CO bound to Mg^{2+} ions. The strongly basic character of the MgO surface explains why CO forms carbonite anions [40–42] or similar structures [43–45] on this oxide. Carbon monoxide is however bonded to Mg^{2+} ions mainly by electrostatic force that is easily removed by evacuation, even at low temperature [46,47].

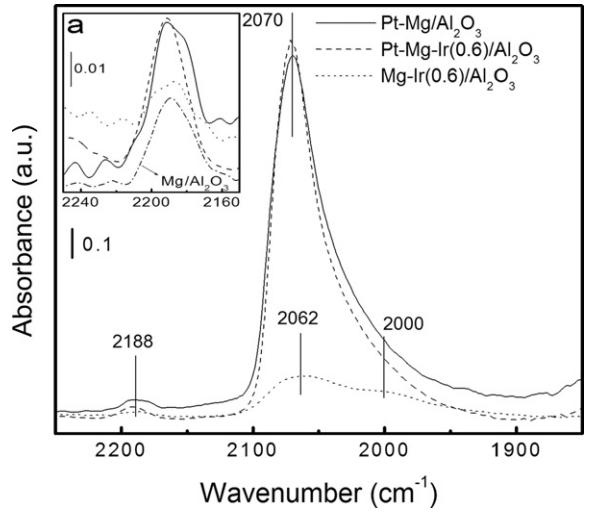

Fig. 4. FTIR spectra of CO adsorbed on some alumina supported catalysts at 30 Torr.

The spectrum of $Pt\text{-}Mg/Al_2O_3$ shows the characteristic absorption peak of Pt^0–CO at 2070 cm^{-1}, while the spectrum of the monometallic $Mg\text{-}Ir(0.6)/Al_2O_3$ catalyst shows an absorption peak at 2062 cm^{-1} and a shoulder about 2000 cm^{-1}, peaks attributed to Ir^0–CO and $Ir^+(CO)_2$ species respectively. Similarly to the $Pt\text{-}Mg/Al_2O_3$, the $Pt\text{-}Mg\text{-}Ir(0.6)/Al_2O_3$ catalyst has a very intense absorption peak at 2070 cm^{-1} due to CO adsorbed on Pt and Ir, both totally reduced to the metallic state. This shows a strong interaction between Pt and Ir. In a previous work we have confirmed the existence of a strong interaction between Pt and Ir on alumina supported catalysts by TEM [20]. It can be seen in Table 2 that incorporation of Ir to the $Pt\text{-}Mg\text{-}Ir(x)$ catalysts produce changes in the metal particle size. A strong decrease in the metal particle size is observed at Ir contents higher than 0.3 wt%. Electron diffraction (ED) experiments of $Pt\text{-}Mg\text{-}Ir(x)$ catalysts suggest the formation of a solid solution between Pt and Ir because crystallographic planes do not resemble pure Pt or pure Ir. These results are consistent with TPR experiments where a strong interaction between Pt and Ir was observed. Moreover they are in agreement with the results of CO FTIR absorption.

Fig. 5 shows the FTIR-CO spectra of the Pt/zeolite, Pt-Ir(0.6)/zeolite and Ir(0.6)/zeolite catalysts. It is widely known that

Table 2
Results of conversion of cyclopentane (CP) and cyclohexane (CH).

Catalyst	CP conversion (5 min), %	CH conversion (mean), %
$Pt\text{-}Mg/Al_2O_3$	6.3	88.0
$Pt\text{-}Mg\text{-}Ir(0.1)/Al_2O_3$	7.2	85.3
$Pt\text{-}Mg\text{-}Ir(0.3)/Al_2O_3$	25.3	76.4
$Pt\text{-}Mg\text{-}Ir(0.6)/Al_2O_3$	61.9	68.0
$Mg\text{-}Ir(0.6)/Al_2O_3$	97.5	46.7
Pt/zeolite	65.6	98.0
Pt-Ir(0.1)/zeolite	70.7	87.7
Pt-Ir(0.3)/zeolite	78.1	81.5
Pt-Ir(0.6)/zeolite	91.4	65.6
Ir(0.6)/zeolite	99.3	25.8

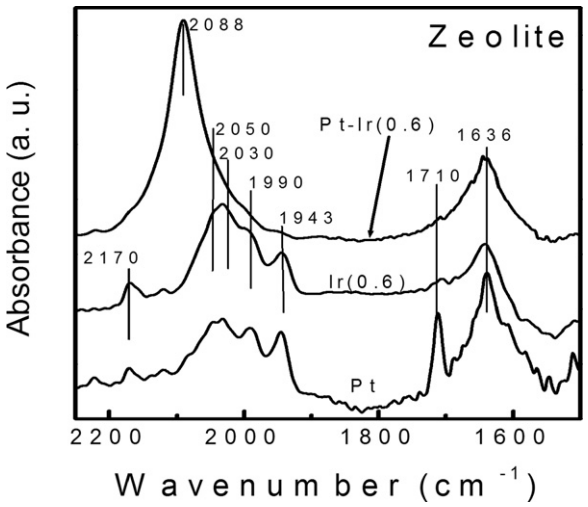

Fig. 5. FTIR spectra of CO adsorbed on some zeolite supported catalysts at 30 Torr.

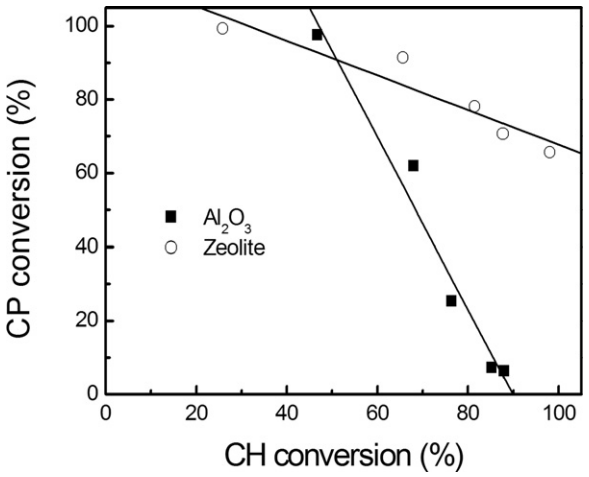

Fig. 6. Cyclopentane conversion as a function of cyclohexane conversion for both catalysts series.

CO adsorption on metal modified zeolites produces several FTIR bands due to the contribution of species associated to the zeolitic structure and with each metal [48]. Some authors have reported results of FTIR absorption of CO on zeolites modified with platinum. For example Jaeger and Schulz-Eldoff [49] have speculated about the existence of two types of Pt particles on Pt/KL zeolite catalysts. The first one would be localized on the outer surface of the zeolite microcrystals or at near surface locations. CO adsorbed on these particles displays absorption bands at 2060–2050 cm^{-1} close to those found in Pt dispersed on conventional supports. The particles of the second group are supposed to be encaged inside zeolite channels so their electronic structure is presumably strongly affected by the surrounding zeolite framework. CO adsorbed on these Pt particles exhibits coverage dependent bands at frequencies in the 1960–1920 cm^{-1} range. The marked downward shift of these CO bands is attributed to the increase of electron density of these particles. Some authors [50–52] suggest that bands at about 2000 cm^{-1} correspond to CO adsorption on well-dispersed small metal particles with great interaction with the support.

Adsorption of CO on $Ir^{3+}Y$ zeolites reportedly does not lead to the formation of carbonyl bands [53] or else it results in a weak band at 2100 cm^{-1} assigned to Ir^{3+}-CO carbonyls [54]. After CO adsorption on hydrogen-reduced samples Bukhardt et al. [53] detected carbonyls on metallic iridium only (a band at 2020 cm^{-1}), but Gelin et al. [55] also reported the formation of two types of $Ir^{+}(CO)_2$ complexes, characterized by pairs of bands at 2088 and 2003 cm^{-1} and 2102 and 2020 cm^{-1}, respectively. Solymosi et al. [33] demonstrated that in addition to a band at 2080–2050 cm^{-1}, a pair of bands at 2107–2090 and 2037–2010 cm^{-1}, due to $Ir^{+}(CO)_2$ complexes, also appears.

The results of Fig. 5 show that the zeolite supported monometallic Pt and Ir catalysts have an absorption peak at about 2050 cm^{-1} attributed to Pt and Ir on the outer surface and three peaks at 2030, 1990 and 1943 cm^{-1} attributed to Pt and Ir particles inside the cage or to Pt particles of high dispersion. Bands in the 1800–1200 cm^{-1} range have been attributed to carbonate species and bands at 1630–1650 cm^{-1} have been assigned to the stretching frequency (ν_{CO}) of bridged carbonates [56]. The band at 1636 cm^{-1} can also be related to the adsorption of CO on the support surface (ν_{CO-OH}), as this band also appears on the reduced HY without any supported metallic particle (not shown).

The spectrum of the bimetallic Pt-Ir(0.6)/zeolite catalyst has a well defined peak at 2088 cm^{-1}. The shift of the peaks to 2088 cm^{-1} clearly points to an alloying effect. Platinum and iridium would be in the metal state and alloyed after the reduction and probably placed outside the zeolite cages [57,58].

It is well known that de/hydrogenation reactions can proceed on simple (monoatomic) sites while hydrogenolysis requires catalytic sites of a more complicated morphology (clusters or ensembles) [59–61]. Pioneering works of Boudart et al. [62,63] on structure sensitivity, classified catalytic reactions as "demanding" (sensitive to morphological structure) and "facile" (structure-insensitive). Demanding reactions would require a particular ensemble of neighboring metal atoms in order to form adsorbate bonds with the proper strength; facile reactions would not. This geometric model has been recently refined to an "ensemble-size" model [64–66] on the assumption that reaction rates are proportional to the probability of finding particular groups of neighboring atoms. In this work two classical test reactions are used that have an entirely different behavior according to the geometric factor theory: cyclopentane (CP) hydrogenolysis (demanding reaction) and cyclohexane (CH) dehydrogenation, which is non-demanding at the reaction conditions used.

The values of conversion of cyclopentane (Table 2) are in agreement with the greater hydrogenolytic activity of Ir in comparison to Pt. The increase of the CP activity as the content of Ir is increased is remarkable in both catalyst series. According to the results of Table 2 the hydrogenolytic activity of the metals supported on alumina is smaller than the activity of the metals supported on the zeolite.

Monometallic Pt deposited on Al_2O_3 or the zeolite has more activity for cyclohexane dehydrogenation than the corresponding Ir catalyst. From the results of Table 2 it could be deduced Ir addition produces the blocking of active sites necessary for CH dehydrogenation. The two series of catalysts show the same activity pattern in relation to this.

Fig. 6 shows results of CP conversion as a function of CH conversion for the alumina and zeolite catalyst series. It can be seen that as the CH conversion increases the CP conversion decreases in both series. This is easily explained considering that CH dehydrogenation is a non-demanding reaction while CP hydrogenolysis is a demanding one. CH conversion would decrease due to the presence of big ensembles of Pt–Ir. These big ensembles are more suitable for CP conversion and hydrogenolysis would be favored.

Table 3 shows the values of conversion and selectivity to i-C_5 and C_1 corresponding to the n-pentane reaction. The catalytic transformation of n-pentane on dual function (metal-acid) catalysts yields many products: (1) isopentane, as a consequence of the bifunctional, acid controlled, isomerization reaction; (2) lighter

Table 3
Final values of n-C_5 conversion and selectivity to C_1 and isomers of C_5. Time-on-stream = 240 min.

Catalyst	X_f, %	$(X_i - X_f)/X_i$	Selectivity to i-C_5, %	Selectivity to C_1, %
Pt-Mg	24.05	0.12	5.58	1.74
Pt-Mg-Ir(0.1)	24.58	0.26	3.52	2.43
Pt-Mg-Ir(0.3)	23.10	0.11	5.95	3.59
Pt-Mg-Ir(0.6)	23.77	0.07	6.48	6.00
Mg-Ir(0.6)	20.01	0.66	3.04	3.57
Pt/zeolite	23.88	0.33	96.41	0.93
Pt-Ir(0.1)/zeolite	32.26	0.61	81.36	0.97
Pt-Ir(0.3)/zeolite	32.73	0.61	80.80	1.41
Pt-Ir(0.6)/zeolite	34.01	0.63	72.97	6.51
Ir(0.6)/zeolite	35.50	0.64	65.47	7.12

Pt-Mg-Ir(x): $T_{reaction}$ = 500 °C; Pt-Ir(x): $T_{reaction}$ = 400 °C; X_f: conversion to 240 min of reaction; X_i: conversion to 5 min of reaction.

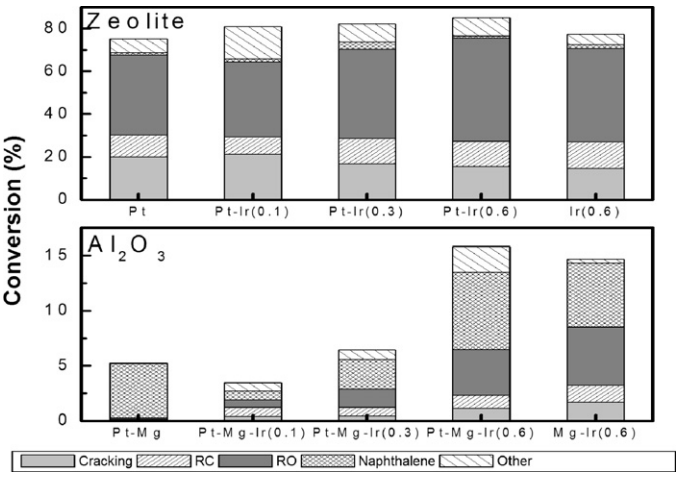

Fig. 7. Products distribution and decalin conversion at 350 °C reaction temperature at 6 h time-on-stream for both catalysts series.

gaseous hydrocarbons (C_2 and C_3), from cracking reactions partly controlled by the metal function and partly by the acidic function; (3) cyclopentane, by dehydro-cyclyzation on metal sites; and (4) methane, from hydrogenolysis on metal sites. No aromatic compounds can be formed during n-C_5 reforming so the main products are paraffin isomers. It is known that the isomerization of n-paraffins proceeds by a bifunctional metal-acid mechanism [67] in which the rate-controlling elementary step takes place on the acid function [68]. Therefore isopentane formation can be considered as an indirect measurement of the acid function activity. The $(X_i - X_f)/X_i$ parameter would be an indication of the deactivation suffered by the catalyst, where X_i and X_f are the initial and final conversion values, respectively. The Pt-Mg-Ir(x)/Al_2O_3 series tested at 500 °C shows less deactivation than the Pt-Ir(x)/zeolite series evaluated at 400 °C. The greater stability of the alumina supported catalysts is related to the stability of the support. Due to its weaker acid strength the alumina support has a lower activity for polymerization of coke precursors. It can also be seen that the catalysts supported on the HY zeolite are more selective for the formation of pentane isomers than the alumina supported ones. This greater selectivity would be due to the higher acidity of the zeolite.

The Pt-Ir(x)/zeolite catalysts evaluated at 500 °C display 100% conversion and very high selectivity to methane (results not shown). This can be explained considering that cracking reactions have high activation energy and therefore the rates of primary and secondary hydrocracking and hydrogenolysis are greatly enhanced at high temperatures. Regarding the relation between the iridium content, acid strength and the selectivity to i-C_5, both series of catalysts show an opposite behavior. In the case of the Pt-Mg-Ir(x)/Al_2O_3 series the selectivity to i-C_5 increases as the amount of strong acid sites increases, while in the Pt-Ir(x)/zeolite series the increase in acid strength enhances the selectivity to cracking products (e.g. methane) at the expense of isomerization.

Pajonk [69] has reported that isomerization catalyzed by bimetallic catalysts is affected by hydrogen spillover. This effect was reported in zeolite supported metal catalysts [70–72]. Setiabudi et al. [73] studied the influence of Ir on H-ZSM-5 supported Pt(0.1 wt%) catalysts and they found that the addition of Ir from 0.3 to 2 wt% decreased the concentration of Lewis and Brønsted acid sites and inhibited the hydrogen induced generation of protonic acid sites (via hydrogen spillover phenomenon). This led to a decrease of the selectivity to i-C_5 and an increase of hydrogenolysis.

Decalin reaction products were classified considering the criterion used by Santikunaporn et al. [13] and Mouli et al. [74]: *cracking products (C_1–C_9 products)*: 2-methyl butane, hexane, 2,3-dimethyl pentane, 3-methylpentane, 5-methyl,1-hexene, methylcyclopentane, propylcyclopentane, 2-methylpropylcyclopentane, 1,1-dimethylcyclopentane, cyclohexane, methylcyclohe-xane, propylcyclohexane, cis 1-ethyl-2-methylcyclohexane, trans 1-ethyl-4-metilcyclohexane, 1-ethyl-3-methylcyclohexane, 1,1,4-trimethylcyclohexane; *ring opening (RO) C_{10} products*: alkylcyclohexanes, alkylcyclopentanes cyclohexenes or benzenes (for example: 1-methyl-2-propylcyclohexane, diethylcyclohexane, cis and trans 1,1,3,5-tetramethylcyclohexane, 2-methylpropylbenzene); *ring contraction (RC) products*: 2,2,3-trimethyl bicyclo[2.2.1]heptane, 2,6,6-trimethyl bicyclo[3.1.1]heptane, 1,1′bicyclopentyl, spiro[4.5]decane, 3,7,7-trimethyl bicycle [4.1.0]heptane; *other products*: 1-methylindan, cis and trans decahydronaphthalene, 1,2-dihydronaphthalene, 1,2,3,4-tetrahydronaphthalene and other heavy dehydrogenation products.

Fig. 7 shows results of decalin conversion and distribution of products obtained at 350 °C. The RO products are mainly alkyl cyclohexanes and alkyl cyclopentanes. The HY supported catalysts are more active than the Pt-Mg-Ir(x)/Al_2O_3 ones. In both series increasing the Ir content increases the selectivity to RO products due to the high hydrogenolytic activity of Ir. The Pt-Ir(x)/zeolite catalysts produce more RO products than the Pt-Mg-Ir(x)/Al_2O_3 ones and this could be due to the higher acidity of the zeolite, especially that of the Brønsted type. In agreement with the results of pyridine TPD, the activity of the Pt-Mg-Ir(x)/Al_2O_3 catalysts increases with acid strength. The alumina supported catalysts produced a higher naphthalene yield than the zeolite supported ones. Among the zeolite catalysts, the Pt-Ir(0.6)/zeolite catalyst is the most suitable catalyst for the ring opening of decalin. It has an adequate metal/acid balance that favors the opening of naphthenic rings.

Table 4 shows the values of conversion, trans/cis decalin ratio and selectivity to ring opening products at 350 and 300 °C and 6 h of time-on-stream. It is important to note that the fed decalin contained 37.5% of the *cis* isomer (1.63 *trans*/*cis* ratio). In both series of catalysts the percentage of *cis*-decalin was lower than the percentage of *trans*-decalin. The high *trans*/*cis* decalin ratio of the products can be mainly due to the occurrence of *cis*-*trans* isomerization and to the greater reactivity of *cis*-decalin in comparison to the *trans* isomer. In both series and at the two reaction temperatures monometallic Ir catalysts produced higher values of the *trans*/*cis* decalin ratio than the corresponding monometallic Pt catalysts. This indicates that *trans* decalin is more easily isomerized to the *cis* form over the Pt catalysts. In this sense Mouli et al. have indicated that stereoisomerization is an important step for the ring opening of decalin [75]. Santikunaporn et al. have reported that *cis*-decalin is much more selective to ring opening products while *cis*-decalin preferentially produces cracking products [13].

Table 4
Decalin conversion at 6 h of time-on-stream and two different reaction temperatures (300 and 350 °C). Selectivity to RO products and trans/cis decalin ratio.

Catalyst	Conversion, %		Selectivity to RO		Trans/cis decalin ratio	
	300 °C	350 °C	300 °C	350 °C	300 °C	350 °C
Pt-Mg/Al_2O_3	1.70	5.26	72.94	2.28	8.04	5.52
Pt-Mg-Ir(0.1)/Al_2O_3	1.50	2.65	86.00	25.28	8.25	6.38
Pt-Mg-Ir(0.3)/Al_2O_3	1.50	6.27	76.67	26.32	7.84	5.23
Pt-Mg-Ir(0.6)/Al_2O_3	1.40	15.78	85.71	26.49	8.14	6.81
Mg-Ir(0.6)/Al_2O_3	2.00	14.66	75.50	36.15	8.06	6.92
Pt/zeolite	65.97	74.29	64.62	50.32	7.91	8.34
Pt-Ir(0.1)/zeolite	43.47	80.82	60.13	43.62	9.91	12.32
Pt-Ir(0.3)/zeolite	45.29	82.05	60.19	50.68	9.21	8.40
Pt-Ir(0.6)/zeolite	75.45	84.85	68.61	56.91	9.56	14.41
Ir(0.6)/zeolite	62.18	77.29	58.73	56.36	12.60	9.00

Trans/cis decalin ratio of the feed = 1.63, *cis*-decalin content of the feed = 37.5%.

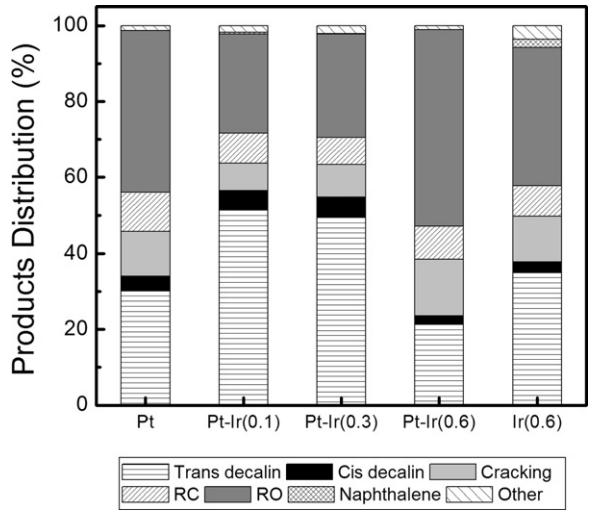

Fig. 8. Products distribution at 300 °C and 6 h time-on-stream. Alumina supported catalysts.

The smaller percentage of *cis*-decalin obtained with the zeolite supported catalysts correlates with the greater yield and selectivity to RO products of these catalysts.

The results of Table 4 indicate that at 300 °C the Pt-Mg-Ir(x)/Al_2O_3 catalysts have a great selectivity to RO products though their activity is very small (conversion < 2%). In the Pt-Ir(x)/zeolite catalyst series the selectivity to RO products is higher at 300 °C than at 350 °C. However it is convenient to operate the reactor at 350 °C in attention to the higher yield of RO products.

Fig. 8 shows the products distribution obtained in the reaction of decalin at 300 °C at 6 h with the Pt-Ir(x)/zeolite catalysts. It can be seen that the contents of naphthalene and other dehydrogenated products is lower at 300 °C than at 350 °C (Fig. 7). It is known that temperatures above 350 °C are not thermodynamically favorable for ring opening. At these temperatures both Pt and Ir catalyze the thermodynamically favored reaction of dehydrogenation [75] of which the presence of naphthalene is an indicator. Moreover the reactivity of *trans*-decalin and the formation of cracking products are enhanced at higher temperatures. At 300 and 350 °C the zeolite catalysts have the same reactivity pattern with respect to the yield of RO products.

4. Conclusions

For both alumina and zeolite supported Pt catalysts the addition of Ir increases the hydrogenolytic activity and decreases the dehydrogenating activity. The test reaction of n-pentane isomerization shows that Ir addition enhances the catalyst stability and the formation of C_5 isomers on the alumina supported catalysts. The opposite occurs with the Pt-Ir/zeolite catalysts. For the two tested catalyst series no correlation was found between the activity for cyclohexane dehydrogenation and the dehydrogenation of decalin to naphthalene.

The catalysts supported on the HY zeolite are significantly more effective for the ring opening of decalin than the Mg doped, alumina supported catalysts. This can be mainly attributed to the higher Brønsted acidity of the zeolite and the higher hydrogenolytic activity of the zeolite supported metal particles. Increasing the Ir content enhances the catalytic activity for formation of ring opening products in both kinds of catalysts. The effect is more noticeable in the Pt-Mg-Ir/Al_2O_3 series.

Among the catalysts tested, Pt-Ir(0.6)/zeolite provides an adequate balance of the metal and acid functions that favors the opening of naphthenic rings.

References

[1] R.C. Santana, P.T. Do, M. Santikunaporn, W.E. Alvarez, J.D. Taylor, E.L. Sughrue, D.E. Resasco, Fuel 85 (2006) 643–656.
[2] F.G.J. Gault, Adv. Catal. 30 (1981) 1–95.
[3] N.T. Tam, R.P. Cooney, G. Curthoys, J. Catal. 44 (1976) 81–86.
[4] Z. Paál, P. Tétényi, Nature 267 (1977) 234–241.
[5] G.B. McVicker, M. Daage, M.S. Touvelle, C.W. Hudson, D.P. Klein, W.C. Baird, B.R. Cook Jr., J.G. Chen, S. Hantzer, D.E.W. Vaughan, E.S. Ellis, O.C. Feeley, J. Catal. 210 (2002) 137–148.
[6] L.M. Kustov, A. Yu Stakheev, T.V. Vasina, O.V. Masloboishchikova, E.G. Khelkovslaya-Sergeeva, P. Zeuthen, Stud. Surf. Sci. Catal. 138 (2001) 307–314.
[7] A. Corma, V. Gonzalez-Alfaro, A.V. Orchillés, J. Catal. 200 (2001) 34–44.
[8] K. Sato, Y. Nishimura, K. Honna, N. Matsubayashi, H. Shimada, J. Catal. 200 (2001) 288–297.
[9] M.A. Arribas, J.J. Mahiques, A. Martínez, Stud. Surf. Sci. Catal. 135 (2001) 303.
[10] M.A. Arribas, A. Martínez, Appl. Catal. A 230 (2002) 203–217.
[11] D. Kubička, N. Kumar, P. Mäki-Arvela, M. Tiitta, V. Niemi, T. Salmi, D. Yu Murzin, J. Catal. 222 (2004) 65–79.
[12] D. Kubicka, N. Kumar, P. Maki-Arvela, M. Tiitta, V. Niemi, H. Karhu, T. Salm, D.Y. Murzin, J. Catal. 227 (2004) 313–327.
[13] M. Santikunaporn, J.E. Herrera, S. Jongpatiwut, D.E. Resasco, W.E. Alvarez, E.L. Sughrue, J. Catal. 228 (2004) 100–113.
[14] M.A. Arribas, P. Concepción, A. Martínez, Appl. Catal. A 267 (2004) 111–119.
[15] J. Barbier, in: G. Ertl, H. Knözinger, J. Wertkamp (Eds.), Handbook of Heterogeneous Catalysis, vol. 1, Wiley-VCH, Veinheim, 1997, p. 257.
[16] C.L. Pieck, P. Marecot, J. Barbier, Appl. Catal. A 134 (1996) 319–329.
[17] C.L. Pieck, C.A. Querini, J.M. Parera, P. Marecot, J. Barbier, Appl. Catal. A 133 (1995) 281–292.
[18] C. Carnevillier, F. Epron, P. Marecot, Appl. Catal. A 275 (2004) 25–33.
[19] V. Pomec, Adv. Catal. 32 (1983) 149–214.
[20] S.A. D'Ippolito, V.M. Benitez, P. Reyes, M.C. Rangel, C.L. Pieck, Catal. Today 172 (2011) 177–182.
[21] W.C. Baird Jr., J.G. Chen, G.B. McVicker, B.Gary, US Patent 6,623,626, 2003.
[22] W.C. Baird Jr., D.P. Klein, J.G. Chen, G.B. McVicker, US Patent 63,683,020, 2004.
[23] C. Carnevillier, F. Epron, P. Marecot, S. Subramanian, J.A. Schwarz, Appl. Catal. A 74 (1991) 65–71.
[24] S.H. Cho, J.S. Park, S.H. Choi, S.H. Kim, J. Power Sources 156 (2006) 260–266.
[25] M. Chiappero, P.T.M. Do, S. Crossley, L.L. Lobban, D.E. Resasco, Fuel 90 (2011) 1155–1165.
[26] K. Chakarova, K. Hadjiivanov, G. Atanasova, K. Tenchev, J. Mol. Catal. A 264 (2007) 270–279.
[27] T. Montanari, O. Marie, M. Daturi, G. Busca, Catal. Today 110 (2005) 339–344.

[28] L. Gutierrez, E. Lombardo, Appl. Catal. A 360 (2009) 107–119.
[29] P. Hollins, Surf. Sci. Rep. 16 (1992) 51–94.
[30] J.A. Anderson, C.H. Rochester, Catal. Today 10 (1991) 275–282.
[31] F. Boccuzzi, G. Ghiotti, A. Chiorino, L. Marchese, Surf. Sci. 233 (1990) 141–152.
[32] J.A. Anderson, M.G.V. Mordente, C.H. Rochester, J. Chem. Soc. Faraday Trans. 1 85 (1989) 2983–2990.
[33] F. Solymosi, E. Novak, A. Molnar, J. Phys. Chem. 94 (1990) 7250–7255.
[34] S.M. Zverev, L.A. Denisenko, A.A. Tsyganenko, Usp. Fotoniki. 9 (1987) 96–101.
[35] A. Tsyganenko, S. Zverev, React. Kinet. Catal. Lett. 36 (1988) 269–274.
[36] C. Morterra, V. Bolis, G. Magnacca, G. Cerrato, J. Electron. Spectrosc. Relat. Phenom. 64–65 (1993) 235–240.
[37] A. Zecchina, E. Platero, C. Otero Arean, J. Catal. 107 (1987) 244–247.
[38] L. Marchese, S. Bordiga, S. Coluccia, G. Martra, A. Zecchina, J. Chem. Soc. Faraday Trans. 89 (1993) 3483–3489.
[39] C. Morterra, V. Bolis, G. Magnacca, Langmuir 10 (1994) 1812–1824.
[40] N. Babaeva, A. Tsyganenko, J. Catal. 123 (1990) 396–416.
[41] M.A. Babaeva, A.A. Tsyganenko, React. Kinet. Catal. Lett. 34 (1987) 9–14.
[42] A. Tarasov, M. Osmanov, V. Schvetz, B. Kazanski, Kinet. Katal. 31 (1990) 645–654.
[43] A. Zecchina, G. Spoto, S. Coluccia, E. Guglielminotti, J. Phys. Chem. 88 (1984) 2575–2581.
[44] M.I. Zaki, H. Knözinger, Mater. Chem. Phys. 17 (1–2) (1987) 201–215.
[45] M. Zaki, H. Knözinger, Spectrochim. Acta A 43 (1987) 1455–1459.
[46] E. Paukshtis, R. Soltanov, E. Yurchenko, React. Kinet. Catal. Lett. 16 (1981) 93–96.
[47] J.W. He, C.A. Estrada, J.S. Corneille, S. Jason, M.C. Wu, D.W. Goodman, Surf. Sci. 261 (1992) 164–170.
[48] K.I. Hadjiivanov, G.N. Vayssilov, Adv. Catal. 47 (2002) 307–511.
[49] N.I. Jaeger, G. Schulz-Eldoff, Catal. Lett. 32 (1995) 147–158.
[50] F. Solymosi, J. Rasko, J. Catal. 62 (1980) 253–263.
[51] F. Solymosi, J. Rasko, J. Catal. 63 (1980) 217–225.
[52] A. Erdohelyi, K. Fodor, G. Suru, Appl. Catal. A 139 (1996) 131–147.
[53] I. Bukhardt, D. Gutschick, H. Landmesser, H. Miessner, in: P.A. Jacobs (Ed.), Proceedings of an International Symposium, vol. 69, Elsevier, Amsterdam, 1991, pp. 215–222.
[54] P. Gelin, G. Goudurier, Y. Ben Taarit, C. Naccache, J. Catal. 70 (1981) 32–40.
[55] P. Gelin, A. Auroux, Y. Ben Taarit, P. Gravelle, Appl. Catal. 46 (1989) 227–240.
[56] F.A. Marchesini, L.B. Gutierrez, C.A. Querini, E.E. Miró, Chem. Eng. J. 159 (2010) 203–211.
[57] C. Mihut, C. Descorme, D. Duprez, M.D. Amiridis, J. Catal. 212 (2002) 125–135.
[58] M.M. Otten, M.J. Clayton, H.H. Lamb, J. Catal. 149 (1994) 211–222.
[59] B. Coq, F. Figueras, J. Catal. 85 (1984) 197–205.
[60] F.H. Ribeiro, A.L. Bonivardi, C. Kim, G.A. Somorjai, J. Catal. 150 (1994) 186–198.
[61] P. Biloen, F.M. Duatzenberg, W.M.H. Sachtler, J. Catal. 50 (1977) 77–86.
[62] M. Boudart, A. Aldag, J.E. Benson, V.A. Dougharty, C.G. Harkings, J. Catal. 6 (1966) 92–99.
[63] M. Boudart, Proceedings of the 6th International Congress of Catalysis, The Chemical Society, London, 1976, p. 1.
[64] W.M.H. Sachtler, R.A. van Santen, Adv. Catal. 26 (1977) 69–119.
[65] R. Coekelbergs, A. Frennet, G. Lienard, P. Resibois, J. Phys. Chem. 39 (1963) 585–591.
[66] J.A. Dalmon, G.A. Martin, J. Catal. 66 (1980) 214–221.
[67] C.A. Querini, N.S. Fígoli, J.M. Parera, Appl. Catal. 52 (1989) 249–262.
[68] V.A. Mazzieri, J.M. Grau, C.R. Vera, J.C. Yori, J.M. Parera, C.L. Pieck, Catal. Today 107 (2005) 643–650.
[69] G.M. Pajonk, Appl. Catal. A 202 (2000) 157–169.
[70] K. Fujimoto, K. Maeda, K. Aimoto, Appl. Catal. A: Gen. 91 (1992) 81–86.
[71] S. Triwahyono, A.A. Jalil, R.R. Mukti, M. Musthofa, N.A.M. Razali, M.A.A. Aziz, Appl. Catal. A 407 (2011) 91–99.
[72] H.D. Setiabudi, A.A. Jalil, S. Triwahyono, N.H.N. Kamarudin, R.R. Mukti, Appl. Catal. A 417-418 (2012) 190–199.
[73] H.D. Setiabudi, A.A. Jalil, S. Triwahyono, J. Catal. 294 (2012) 128–135.
[74] K.C. Mouli, V. Sundaramurthy, A.K. Dalai, J. Mol. Catal. A: Chem. 304 (2009) 77–84.
[75] K.C. Mouli, V. Sundaramurthy, A.K. Dalai, Z. Ring, Appl. Catal. A 321 (2007) 17–26.